

From approximating subdivision schemes for exponential splines to high-performance interpolating algorithms

L. Romani ^{a,*}

^a*Department of Mathematics and Applications, University of Milano-Bicocca,
Via R. Cozzi 53, 20125 Milano, Italy*

Abstract

In this work we construct three novel families of approximating subdivision schemes that generate piecewise exponential polynomials and we show how to convert these into interpolating schemes of great interest in curve design for their ability to reproduce important analytical shapes and to provide highly smooth limit curves with a controllable tension.

In particular, throughout this paper we will focus on the derivation of 6-point interpolating schemes that turn out to be unique in combining vital ingredients like C^2 -continuity, simplicity of definition, ease of implementation, user independency, tension control and ability to reproduce salient trigonometric and transcendental curves.

Key words: Binary subdivision; Laurent polynomial formalism; Interpolation; Analytical shapes reproduction; Tension control.

MSC: 65D17; 65D07; 65D05.

1 Introduction

The main interest in the study of curve subdivision has always been the development of easy-to-use techniques that can make the construction of curves more flexible and efficient.

Starting from the idea that interpolatory methods have the ability to generate curves in a very predictable manner (due to the fact that the produced limit shapes pass

* Corresponding author.

Email address: `lucia.romani@unimib.it` (L. Romani).

through the given control points), research is continually moving toward the investigation of interpolatory refinement rules able to combine the greatest number of features considered vital or simply desirable in curve design. However, although the recent burgeoning literature in the field, there are still no available proposals able to guarantee curvature-continuous limit shapes possessing properties like tension control and important analytical curves reproduction. In fact, while the interpolatory schemes presented in [2] and [19] are C^2 -continuous, they cannot represent any kind of fundamental shapes except cubic polynomials, and while the schemes in [8] and [1], [20], [21] can respectively reproduce circles and conic sections, they are only C^1 -continuous.

In this paper we will therefore address the definition of interpolating 6-point C^2 schemes including in the refinement equations a non-stationary parameter that, besides offering the possibility of intuitively modifying the tension of the limit shape, allows reproducing several trigonometric and transcendental curves often needed in CAGD and its applications.

To come to their rules, in Section 2 we will introduce non-stationary approximating schemes that allow an exact representation of functions from spaces combining algebraic and exponential polynomials. Then, in Section 3 we will show how these new proposals can be converted into 2ℓ -point interpolating schemes reproducing the same function spaces, and finally, in Section 4 we will exploit this constructive approach to derive high-performance interpolating 6-point schemes with outstanding reproducing properties. Some examples aimed at illustrating the main features of the proposed algorithms will be shown in Section 5.

2 Non-stationary approximating schemes for exponential splines

In curve subdivision we start with an initial polyline $P^0 = \{p_j^0\}_{j \in \mathbb{Z}^+}$, and in each step we insert new vertices calculated as linear combinations of the existing ones and we connect them with edges, producing a refined polyline $P^{k+1} = \{p_j^{k+1}\}_{j \in \mathbb{Z}^+}$, $k \geq 0$. In approximating schemes, in each step we also adjust the old vertices, again as linear combinations of the existing points. If the weights of the linear combinations change at each round of refinement, the subdivision scheme is called non-stationary, and a superscript k is added to denote the dependence on the subdivision level. The information about these linear combinations is generally coded in the mask of the scheme. In the following we will denote by σ^k the non-stationary mask with coefficients $\{\sigma_j^k\}_{j \in \mathbb{Z}^+}$ and by $\sigma^k(z) = \sum_{j \in \mathbb{Z}^+} \sigma_j^k z^j$ the generating function (or Laurent polynomial) of the respective sequence. In this way, using the generating function of p_j^k and p_j^{k+1} , the formal relation between points at two successive refinement levels can be written in the generating function form as $P^{k+1}(z) = \sigma^k(z)P^k(z^2)$, with $P^k(z) = \sum_{j \in \mathbb{Z}^+} p_j^k z^j$, $k \geq 0$.

The purpose of this section is to introduce the Laurent polynomial representations of non-stationary approximating schemes characterized by the property of reprodu-

cing functions from spaces combining algebraic and exponential polynomials. To this aim we will start out defining the general finite-dimensional space of exponential polynomials and then we will focus on the Laurent polynomial formalism of approximating schemes whose limit functions belong to subclasses of L-splines [16] that allow an exact representation of the considered spaces.

Definition 1 Let $\{\gamma_j\}_{j=0}^M$ with $\gamma_M \neq 0$, $M \in \mathbb{Z}^+$, be a finite set of real or imaginary numbers, and let D^j be the j -th order differentiation operator. We denote by V_M the subspace

$$V_M = \left\{ \phi : \mathbb{R} \rightarrow \mathbb{C}, \phi \in C^M(\mathbb{R}) : \sum_{j=0}^M \gamma_j D^j \phi = 0 \right\}.$$

Define $\gamma(z) = \sum_{j=0}^M \gamma_j z^j$ and let $\{(\theta_i, \varrho_i)\}_{i=1, \dots, N}$ be the set of zeros with multiplicities of $\gamma(z) = 0$,

$$\begin{aligned} \gamma^{(r_i)}(\theta_i) &= 0, & \forall r_i = 0, \dots, \varrho_i - 1, & \quad i = 1, \dots, N \\ \varrho_i &\in \mathbb{N}, & M &= \sum_{i=1}^N \varrho_i. \end{aligned} \tag{1}$$

Then V_M is the subspace of dimension M of exponential polynomials of the form

$$V_M = \text{span}\{x^{r_i} e^{\theta_i x} : r_i = 0, \dots, \varrho_i - 1, i = 1, \dots, N\}.$$

In [18] it was proved that any non-stationary approximating scheme with a symbol of the form

$$\sigma^k(z) = 2 \prod_{i=1}^N \prod_{r_i=0}^{\varrho_i-1} \frac{e^{\frac{\theta_i}{2^{k+1}}} z + 1}{e^{\frac{\theta_i}{2^{k+1}}} + 1}, \quad k \geq 0, \tag{2}$$

generates limit functions belonging to the subclass of C^{M-2} L-splines whose pieces are exponentials of the space V_M .

In the following subsections we construct three novel families of non-stationary approximating schemes whose symbols can be written in the form (2), thus allowing the reproduction of piecewise exponential polynomials.

2.1 A family of approximating subdivision schemes reproducing functions in the space $\{1, x, \dots, x^{n-1}, x^n, e^{tx}, e^{-tx}\}$

We start out focussing our attention on the family of approximating schemes identified by the Laurent representation

$$\sigma^k(z) = \frac{1}{2^n} (z+1)^{n+1} \frac{z^2 + 2v^{k+1}z + 1}{2(v^{k+1} + 1)}. \quad (3)$$

Assuming that n is an arbitrary integer larger than or equal to 1, and v^{k+1} a parameter updated at each step $k \geq 0$ through the recurrence

$$v^{k+1} = \sqrt{\frac{1 + v^k}{2}}, \quad (4)$$

the following result holds.

Proposition 2 *Let t denote a non-negative real or imaginary constant, namely let $t = 0$, $t = s$ or $t = is$, with $s > 0$.*

The approximating scheme with symbol (3), where $n \in \mathbb{N}$ and v^{k+1} is updated through (4), reproduces functions in the space $V_{n+3,t} \equiv \{1, x, \dots, x^{n-1}, x^n, e^{tx}, e^{-tx}\}$, i.e. it reproduces C^{n+1} exponential polynomial B-splines.

PROOF. The related proof follows by the fact that the parameter v^{k+1} defined through recurrence (4) satisfies the equality

$$v^{k+1} = \frac{1}{2}(e^{t_{k+1}} + e^{-t_{k+1}}) \quad (5)$$

with $t_{k+1} = \frac{t}{2^{k+1}}$ (see [1]). Hence, due to (5), the Laurent polynomial $\sigma^k(z)$ in (3) can be rewritten in the form

$$\sigma^k(z) = \frac{1}{2^n} (z+1)^{n+1} \frac{e^{t_{k+1}}z + 1}{e^{t_{k+1}} + 1} \frac{e^{-t_{k+1}}z + 1}{e^{-t_{k+1}} + 1}. \quad (6)$$

We now observe that, denoted with $\{\theta_i\}_{i=1,2,3}$ the set of values $\theta_1 = 0$, $\theta_2 = t$, $\theta_3 = -t$, with multiplicities $\varrho_1 = n+1$, $\varrho_2 = \varrho_3 = 1$, we can further rewrite (6) as in (2), thus obtaining

$$\sigma^k(z) = 2 \prod_{i=1}^3 \prod_{r_i=0}^{\varrho_i-1} \frac{e^{\frac{\theta_i}{2^{k+1}}z} + 1}{e^{\frac{\theta_i}{2^{k+1}}} + 1}. \quad (7)$$

Since $\{(\theta_i, \varrho_i)\}_{i=1,2,3}$ identifies the set of zeros with multiplicities of the polynomial equation $z^{n+3} - t^2 z^{n+1} = 0$ associated with the differential equation $\phi^{(n+3)}(z) - t^2 \phi^{(n+1)}(z) = 0$, it follows that the limit functions for the scheme (3)-(4) are C^{n+1} exponential polynomial B-splines whose pieces are functions of the space $V_{n+3,t}$. \square

Corollary 3 *Directly from Proposition 2 we thus know that the subdivision scheme (3)-(4)*

- *reproduces functions in the space*

$$V_{n+3, \text{is}} \equiv \{1, x, \dots, x^{n-1}, x^n, \cos(sx), \sin(sx)\},$$

i.e. generates C^{n+1} trigonometric polynomial B-splines ([3], [14]), whenever $v^0 \in (-1, 1)$, that is $t = \text{is}$, $s > 0$;

- *reproduces functions in the space*

$$V_{n+3,0} \equiv \{1, x, \dots, x^{n+1}, x^{n+2}\},$$

i.e. generates C^{n+1} polynomial B-splines, whenever $v^0 = 1$, that is $t = 0$;

- *reproduces functions in the space*

$$V_{n+3,s} \equiv \{1, x, \dots, x^{n-1}, x^n, \cosh(sx), \sinh(sx)\},$$

i.e. generates C^{n+1} hyperbolic polynomial B-splines ([11], [12]), whenever $v^0 \in (1, +\infty)$, that is $t = s > 0$.

Remark 4 *Note that the scheme with symbol in (3), if modified by replacing v^{k+1} with v_i^{k+1} , defines a scheme reproducing the very general class of UE-splines recently introduced in [17]. In fact, being the shape parameter v_i^{k+1} updated through (4) for all $k \geq 0$ as well as variable with the choice of i , it allows representing spline curves defined over spaces containing simultaneously polynomial, trigonometric and hyperbolic functions, as the parameter t_i , introduced in correspondence of each curve segment, may be indifferently chosen as 0 , s or is , for an arbitrary $s > 0$.*

In the following subsections we will introduce two other novel families of approximating schemes whose symbols are still enclosed in the form (2). They are both featured by C^{2n} smoothness, but they allow an exact representation of functions from spaces that differently mix algebraic and exponential polynomials.

2.2 *A family of approximating subdivision schemes reproducing functions in the space $\{1, x, e^{tx}, e^{-tx}, \dots, e^{ntx}, e^{-ntx}\}$*

Let $\lambda_j(v^{k+1}) = \det(L)$, where L denotes the $j \times j$ tridiagonal matrix

$$L = \begin{bmatrix} 2v^{k+1} & 1 & 0 & 0 & \cdots & 0 \\ 2 & 2v^{k+1} & 1 & 0 & \cdots & 0 \\ 0 & 1 & 2v^{k+1} & 1 & \cdots & \vdots \\ 0 & 0 & 1 & 2v^{k+1} & \ddots & 0 \\ \vdots & \vdots & \vdots & \ddots & \ddots & 1 \\ 0 & 0 & 0 & \cdots & 1 & 2v^{k+1} \end{bmatrix} \in \mathbb{R}^{j \times j}. \quad (8)$$

We consider the non-stationary symbol

$$\sigma^k(z) = \frac{1}{2} (z+1)^2 \prod_{j=1}^n \frac{z^2 + \lambda_j(v^{k+1})z + 1}{\lambda_j(v^{k+1}) + 2} \quad (9)$$

where $n \in \mathbb{N}$ and v^{k+1} is updated at each step $k \geq 0$ through the recurrence formula (4). Hence the following result holds.

Proposition 5 *Let t denote a non-negative real or imaginary constant, namely let $t = 0$, $t = s$ or $t = is$, with $s > 0$.*

The approximating scheme with symbol (9), where $n \in \mathbb{N}$ and v^{k+1} is updated through (4), reproduces functions in the space $V_{2n+2,t} \equiv \{1, x, e^{tx}, e^{-tx}, \dots, e^{ntx}, e^{-ntx}\}$, i.e. it reproduces a special subclass of C^{2n} L -splines.

PROOF. The related proof follows by the fact that, as previously observed, the parameter v^{k+1} defined as in (4) satisfies the equality (5) with $t_{k+1} = \frac{t}{2^{k+1}}$ for all $k \geq 0$. Hence, due to (5), the Laurent polynomial $\sigma^k(z)$ in (9) can be rewritten in the form

$$\sigma^k(z) = \frac{1}{2} (z+1)^2 \frac{e^{t_{k+1}z} + 1}{e^{t_{k+1}} + 1} \frac{e^{-t_{k+1}z} + 1}{e^{-t_{k+1}} + 1} \cdots \frac{e^{nt_{k+1}z} + 1}{e^{nt_{k+1}} + 1} \frac{e^{-nt_{k+1}z} + 1}{e^{-nt_{k+1}} + 1}. \quad (10)$$

We now observe that, denoted with $\{\theta_i\}_{i=1, \dots, 2n+1}$ the set of values $\theta_1 = 0$, $\theta_{2j} = jt$, $\theta_{2j+1} = -jt$ ($j = 1, \dots, n$), with multiplicities $\varrho_1 = 2$, $\varrho_i = 1$ ($i = 2, \dots, 2n+1$), we can further rewrite (10) in the form (2), thus obtaining

$$\sigma^k(z) = 2 \prod_{i=1}^{2n+1} \prod_{r_i=0}^{\varrho_i-1} \frac{e^{\frac{\theta_i}{2^{k+1}}z} + 1}{e^{\frac{\theta_i}{2^{k+1}}} + 1}. \quad (11)$$

Assuming the notations $\mu^0 = 1$, $\nu^n = (1, -n^2 t^2)$ and $\mu^n = \{\mu_h^n\}_{h=1, \dots, n+1} \forall n \geq 1$ with

$$\mu_h^n = (\mu^{n-1} \otimes \nu^n)_h = \sum_{i+j=h} \mu_i^{n-1} \nu_j^n, \quad h = 1, \dots, n+1, \quad (12)$$

it turns out that $\{(\theta_i, \varrho_i)\}_{i=1, \dots, 2n+1}$ identifies the set of zeros with multiplicities of the polynomial equation $z^2 \sum_{h=1}^{n+1} \mu_h^n z^{2n+2-2h} = 0$ associated with the differential equation $\phi^{(2)}(z) \sum_{h=1}^{n+1} \mu_h^n \phi^{(2n+2-2h)}(z) = 0$. Hence it follows that the limit functions for the scheme (9)-(4) belong to the special subclass of C^{2n} L-splines [16] reproducing functions from the space $V_{2n+2,t}$. \square

Corollary 6 *Directly from the proof of Proposition 5 we thus know that the subdivision scheme (9)-(4)*

- *reproduces functions in the space*

$$V_{2n+2, is} \equiv \{1, x, \cos(sx), \sin(sx), \dots, \cos(nsx), \sin(nsx)\},$$

i.e. generates C^{2n} mixed trigonometric splines ([13], [16]) whenever $v^0 \in (-1, 1)$, that is $t = is$, $s > 0$;

- *reproduces functions in the space*

$$V_{2n+2, 0} \equiv \{1, x, \dots, x^{2n}, x^{2n+1}\},$$

i.e. generates C^{2n} polynomial B-splines whenever $v^0 = 1$, that is $t = 0$;

- *reproduces functions in the space*

$$V_{2n+2, s} \equiv \{1, x, \cosh(sx), \sinh(sx), \dots, \cosh(nsx), \sinh(nsx)\},$$

i.e. generates C^{2n} splines-in-tension [16] whenever $v^0 \in (1, +\infty)$, that is $t = s > 0$.

2.3 *A family of approximating subdivision schemes reproducing functions in the space $\{1, x, e^{tx}, e^{-tx}, \dots, x^{n-1}e^{tx}, x^{n-1}e^{-tx}\}$*

We finally consider the symbol

$$\sigma^k(z) = \frac{1}{2} (z+1)^2 \frac{(z^2 + 2v^{k+1}z + 1)^n}{2^n(v^{k+1} + 1)^n} \quad (13)$$

where $n \in \mathbb{N}$ and v^{k+1} is updated at each step $k \geq 0$ through the recurrence formula (4). Hence the following result holds.

Proposition 7 *Let t denote a non-negative real or imaginary constant, namely let $t = 0$, $t = s$ or $t = is$, with $s > 0$.*

The approximating scheme with symbol (13), where $n \in \mathbb{N}$ and v^{k+1} is updated through (4), reproduces functions in the space $V_{2n+2,t} \equiv \{1, x, e^{tx}, e^{-tx}, xe^{tx}, xe^{-tx}, \dots, x^{n-1}e^{tx}, x^{n-1}e^{-tx}\}$, i.e. it reproduces a special subclass of C^{2n} L-splines.

PROOF. The related proof follows by the fact that, as previously observed, the parameter v^{k+1} defined as in (4) satisfies the equality (5) with $t_{k+1} = \frac{t}{2^{k+1}}$ for all $k \geq 0$. Hence, due to (5), the Laurent polynomial $\sigma^k(z)$ in (13) can be rewritten in the form

$$\sigma^k(z) = \frac{1}{2}(z+1)^2 \frac{(e^{t_{k+1}}z+1)^n}{(e^{t_{k+1}}+1)^n} \frac{(e^{-t_{k+1}}z+1)^n}{(e^{-t_{k+1}}+1)^n}. \quad (14)$$

We now observe that, denoted with $\{\theta_i\}_{i=1,2,3}$ the set of values $\theta_1 = 0$, $\theta_2 = t$, $\theta_3 = -t$, with multiplicities $\varrho_1 = 2$, $\varrho_2 = \varrho_3 = n$, we can further rewrite (14) as in (2), thus obtaining

$$\sigma^k(z) = 2 \prod_{i=1}^3 \prod_{r_i=0}^{\varrho_i-1} \frac{e^{\frac{\theta_i}{2^{k+1}}z+1}}{e^{\frac{\theta_i}{2^{k+1}}+1}}. \quad (15)$$

Since $\{(\theta_i, \varrho_i)\}_{i=1,2,3}$ identifies the set of zeros with multiplicities of the polynomial equation $z^2(z^2-t^2)^n = 0$ associated with the differential equation $\phi^{(2)}(z)(\phi^{(2)}(z)-t^2)^n = 0$, it follows that the limit functions for the scheme (13)-(4) belong to the special subclass of C^{2n} L-splines [16] reproducing functions in the space $V_{2n+2,t}$. \square

Corollary 8 *Directly from the proof of Proposition 7 we thus know that the subdivision scheme (13)-(4)*

- *reproduces functions in the space*

$$V_{2n+2, is} \equiv \{1, x, \cos(sx), \sin(sx), \dots, x^{n-1} \cos(sx), x^{n-1} \sin(sx)\},$$

i.e. generates C^{2n} mixed trigonometric splines ([13], [16]), whenever $v^0 \in (-1, 1)$, that is $t = is$, $s > 0$;

- *reproduces functions in the space*

$$V_{2n+2, 0} \equiv \{1, x, \dots, x^{2n}, x^{2n+1}\},$$

i.e. generates C^{2n} polynomial B-splines, whenever $v^0 = 1$, that is $t = 0$;

- *reproduces functions in the space*

$$V_{2n+2, s} \equiv \{1, x, \cosh(sx), \sinh(sx), \dots, x^{n-1} \cosh(sx), x^{n-1} \sinh(sx)\},$$

i.e. generates C^{2n} splines-in-tension [16], whenever $v^0 \in (1, +\infty)$, that is $t = s > 0$.

3 From exponentials reproducing approximating schemes to 2ℓ -point interpolating schemes with the same reproduction properties

In [10] it was observed that the Dubuc-Deslauriers interpolating 4-point scheme ([5], [6]) can be derived from the cubic B-spline scheme through a sequence of weighted averaging operations. In this work such a relation will be rewritten in terms of their Laurent polynomial representations and extended to their non-stationary versions ([1] and [15]). Furthermore, we will show that, from any approximating scheme able to reproduce functions in a given space of exponential polynomials $V_{2\ell,t}$ (with $t = 0$, $t = s$, or $t = is$, $s > 0$), a 2ℓ -point interpolating scheme with the same reproduction properties can be derived straightforwardly via its Laurent polynomial representation. To this aim we recall that, exploiting only non-negative powers of z , a 2ℓ -point interpolatory scheme is defined by a Laurent polynomial of degree $4\ell - 2$ whose coefficients for the odd powers of z are all zero except that of $z^{2\ell-1}$ which is equal to 1 ([5], [6]). Thus, taking a degree- 2ℓ symbol of an approximating scheme $\sigma^k(z)$, it is easy to see that, if we introduce a degree- $(2\ell - 2)$ polynomial $\omega^k(z)$ of the form

$$\omega^k(z) = \sum_{j=0}^{2(\ell-1)} \omega_j^k z^j, \quad \text{with } \omega_j^k = \omega_{2(\ell-1)-j}^k \quad \forall j = 0, \dots, \ell - 2, \quad (16)$$

whenever the coefficients $\{\omega_j^k\}_{j=0, \dots, \ell-1}$ are determined by solving the linear system

$$\begin{cases} \sigma_1^k \omega_0^k + \sigma_0^k \omega_1^k = 0 \\ \sigma_3^k \omega_0^k + (\sigma_2^k + \sigma_0^k) \omega_1^k + \sigma_1^k \omega_2^k = 0 \\ \vdots \\ \sigma_{2\ell-5}^k \omega_0^k + (\sigma_{2\ell-6}^k + \sigma_0^k) \omega_1^k + \dots + (\sigma_{\ell-2}^k + \sigma_{\ell-4}^k) \omega_{\ell-3}^k + \sigma_{\ell-3}^k \omega_{\ell-2}^k = 0 \\ \sigma_{2\ell-3}^k \omega_0^k + (\sigma_{2\ell-4}^k + \sigma_0^k) \omega_1^k + \dots + (\sigma_{\ell-1}^k + \sigma_{\ell-3}^k) \omega_{\ell-2}^k + \sigma_{\ell-2}^k \omega_{\ell-1}^k = 0 \\ 2\omega_0^k + 2\omega_1^k + \dots + 2\omega_{\ell-2}^k + \omega_{\ell-1}^k = 1, \end{cases} \quad (17)$$

the polynomial

$$\zeta^k(z) = \sigma^k(z) \omega^k(z) \quad (18)$$

will define a 2ℓ -point interpolatory scheme (in fact, the first $\ell - 1$ equations in (17) correspond to conditions $\zeta_{2j-1}^k = \zeta_{4\ell-2j-1}^k = 0 \quad \forall j = 1, \dots, \ell - 1$, and the last one to

$\sum_{j=0}^{2(\ell-1)} \omega_j^k = 1$, namely $\zeta_{2\ell-1}^k = 1$).

In the following Proposition we will show that, taken a degree- 2ℓ polynomial $\sigma^k(z)$ featured by the property of reproducing functions from a certain space $V_{2\ell,t}$, the 2ℓ -point interpolatory scheme with symbol $\zeta^k(z)$ in (18) will possess the same reproduction property.

To this purpose we introduce the following Lemma.

Lemma 9 *The degree- $(2\ell - 2)$ Laurent polynomial $\omega^k(z)$ in (16) is univocally defined by coefficients*

$$\omega_j^k = \frac{(-1)^{\ell-j-1} \det(\hat{S}_{\ell,j+1}^k)}{\det(S_\ell^k)} \quad j = 0, \dots, \ell - 1 \quad (19)$$

where S_ℓ^k is the $\ell \times \ell$ lower Hessenberg matrix

$$S_\ell^k = \begin{bmatrix} \sigma_1^k & \sigma_0^k & 0 & 0 & 0 & \dots & 0 \\ \sigma_3^k & \sigma_2^k + \sigma_0^k & \sigma_1^k & 0 & 0 & \dots & 0 \\ \sigma_5^k & \sigma_4^k + \sigma_0^k & \sigma_3^k + \sigma_1^k & \sigma_2^k & 0 & \dots & 0 \\ \vdots & \vdots & \dots & \vdots & \ddots & \ddots & \vdots \\ \sigma_{2\ell-5}^k & \sigma_{2\ell-6}^k + \sigma_0^k & \dots & \sigma_{\ell-1}^k + \sigma_{\ell-5}^k & \sigma_{\ell-2}^k + \sigma_{\ell-4}^k & \sigma_{\ell-3}^k & 0 \\ \sigma_{2\ell-3}^k & \sigma_{2\ell-4}^k + \sigma_0^k & \dots & \sigma_{\ell+1}^k + \sigma_{\ell-5}^k & \sigma_\ell^k + \sigma_{\ell-4}^k & \sigma_{\ell-1}^k + \sigma_{\ell-3}^k & \sigma_{\ell-2}^k \\ \dots & \dots & \dots & \dots & \dots & \dots & \dots \end{bmatrix} \quad (20)$$

and $\hat{S}_{\ell,j+1}^k$ denotes the $(\ell - 1) \times (\ell - 1)$ matrix obtained by eliminating column $j + 1$ from the $(\ell - 1) \times \ell$ submatrix of S_ℓ^k corresponding to its first $\ell - 1$ rows, here denoted by \hat{S}_{ℓ}^k .

PROOF. Since the linear system in (17) can be rewritten in the following matrix form

$$S_\ell^k \begin{bmatrix} \omega_0^k \\ \omega_1^k \\ \vdots \\ \omega_{\ell-2}^k \\ \omega_{\ell-1}^k \end{bmatrix} = \begin{bmatrix} 0 \\ 0 \\ \vdots \\ 0 \\ 1 \end{bmatrix},$$

where S_ℓ^k is the $\ell \times \ell$ lower Hessenberg matrix in (20), it turns out that (17) has a unique solution due to non-singularity of the coefficients matrix. In particular, it can be shown by induction on ℓ , that it is given by the explicit formula (19). \square

Proposition 10 *Let $\sigma^k(z)$ be the degree- 2ℓ Laurent polynomial of an approximating scheme reproducing functions from the space $V_{2\ell,t}$. Then the 2ℓ -point interpolating scheme $\zeta^k(z)$ with symbol in (18), reproduces functions from the same space $V_{2\ell,t}$.*

PROOF. Let $z_{i,k+1} = e^{-\frac{\theta_i}{2^{k+1}}}$, $i = 1, \dots, N$. Since by results in [18] $\sigma^k(z)$ is a polynomial of the form

$$\sigma^k(z) = 2 \prod_{i=1}^N \prod_{r_i=0}^{\varrho_i-1} \frac{e^{\frac{\theta_i}{2^{k+1}}} z + 1}{e^{\frac{\theta_i}{2^{k+1}}} + 1} \quad \text{with} \quad \sum_{i=1}^N \varrho_i = 2\ell,$$

it is easy to verify that the following equalities turn out to be satisfied:

$$\begin{aligned} \sigma^k(-z_{i,k+1}) &= 0, & \forall i &= 1, \dots, N \\ \frac{d^{r_i}}{dz^{r_i}} \sigma^k(-z_{i,k+1}) &= 0, & \forall r_i &= 1, \dots, \varrho_i - 1, \quad i = 1, \dots, N. \end{aligned} \quad (21)$$

Thus, by (18), it is also

$$\begin{aligned} \zeta^k(-z_{i,k+1}) &= 0, & \forall i &= 1, \dots, N \\ \frac{d^{r_i}}{dz^{r_i}} \zeta^k(-z_{i,k+1}) &= 0, & \forall r_i &= 1, \dots, \varrho_i - 1, \quad i = 1, \dots, N. \end{aligned} \quad (22)$$

Now, introducing $\tilde{\zeta}^k(z) = \zeta^k(z) z^{-(2\ell-1)}$ and exploiting Lemma 9, it can be shown that equations

$$\begin{aligned} \tilde{\zeta}^k(z_{i,k+1}) &= 2, & \forall i &= 1, \dots, N \\ \frac{d^{r_i}}{dz^{r_i}} \tilde{\zeta}^k(z_{i,k+1}) &= 0, & \forall r_i &= 1, \dots, \varrho_i - 1, \quad i = 1, \dots, N \end{aligned} \quad (23)$$

are satisfied for any arbitrary ℓ .

Hence, as equalities (22)-(23) turn out to be simultaneously true, recalling Theorem 2.3 in [7] we can claim that the interpolating scheme $\zeta^k(z)$ reproduces $V_{2\ell,t}$. \square

Corollary 11 *When $n = 2\ell - 3$, the polynomial $\sigma^k(z)$ in (3) turns out to have degree 2ℓ . Hence by computing (18) with $\omega^k(z)$ as in (16)-(19), we define a 2ℓ -point interpolating scheme reproducing functions from the space*

$$V_{2\ell,t} \equiv \{1, x, \dots, x^{2\ell-4}, x^{2\ell-3}, e^{tx}, e^{-tx}\}.$$

When $n = \ell - 1$, the polynomial $\sigma^k(z)$ in (9) turns out to have degree 2ℓ . Hence by computing (18) with $\omega^k(z)$ as in (16)-(19), we define a 2ℓ -point interpolating scheme reproducing functions from the space

$$V_{2\ell,t} \equiv \{1, x, e^{tx}, e^{-tx}, \dots, e^{(\ell-1)tx}, e^{-(\ell-1)tx}\}.$$

When $n = \ell - 1$, the polynomial $\sigma^k(z)$ in (13) turns out to have degree 2ℓ . Hence by computing (18) with $\omega^k(z)$ as in (16)-(19), we define a 2ℓ -point interpolating

scheme reproducing functions from the space

$$V_{2\ell,t} \equiv \{1, x, e^{tx}, e^{-tx}, xe^{tx}, xe^{-tx}, \dots, x^{\ell-2}e^{tx}, x^{\ell-2}e^{-tx}\}.$$

Corollary 12 *As concerns the 2ℓ -point interpolating schemes derived in Corollary 11, whenever we take an initial polyline made of points $\{p_j^0\}_{j \in \mathbb{Z}^+}$ lying equidistant in the parameter $u > 0$ on a curve from the corresponding space $V_{2\ell,t}$ (with $t = 0$, $t = s$ or $t = is$, $s > 0$), by setting the initial parameter $v^0 = \frac{1}{2}(e^{tu} + e^{-tu})$ we are able to reproduce the curve from which those points are sampled (see Figures 2, 3, 4, 5, 6, 7).*

Corollary 13 *Both as concerns the approximating schemes $\sigma^k(z)$ in (3), (9), (13) and the associated 2ℓ -point interpolating schemes $\zeta^k(z)$ derived in Corollary 11, the starting parameter $v^0 \in (-1, +\infty)$ affects the behaviour of the limit curve in such a way that, the greater it is, the smaller is the distance of the resulting shape from the starting polyline (see Figures 8, 9, 10).*

4 High-performance interpolating 6-point C^2 subdivision schemes

Let us start by observing that when $\ell = 2$ (i.e. $n = 1$), the polynomial $\sigma^k(z)$ in (3) becomes the Laurent polynomial of the subdivision scheme reproducing C^2 cubic exponential B-splines [15]. Computing coefficients $\{\omega_j^k\}_{j=0,1}$ of $\omega^k(z)$ as in (19), we get $\omega_0^k = -\frac{1}{2v^{k+1}}$, $\omega_1^k = \frac{v^{k+1}+1}{v^{k+1}}$. Hence, assuming v^{k+1} to be updated at each step by equation (4), the generating function $\zeta^k(z)$ turns out to be the symbol of the 4-point interpolating scheme introduced in [1], which allows reproducing functions from the space $V_{4,t} = \{1, x, e^{tx}, e^{-tx}\}$ with $t = 0$, $t = s$, or $t = is$, for any $s > 0$. Therefore, whenever $t = is$, $s > 0$, for any subdivision level $k \geq 0$ the recurrence relation in (4) defines a parameter $v^{k+1} = \cos\left(\frac{s}{2^{k+1}}\right)$, with $s \in [0, \pi)$. In this case, the generating function $\zeta^k(z)$ corresponds to the symbol of the 4-point interpolating scheme described in [8] as well as in [4]. As a consequence (differently from what claimed in the latter) such a scheme can only reproduce functions from the space $V_{4,is} = \{1, x, \cos(sx), \sin(sx)\}$, for a given angle $s \in [0, \pi)$, namely it allows representing only the subclass of mixed trigonometric functions containing just a sine and a cosine with such a fixed argument. For this reason, curves like the cardioid or the astroid, since defined by the parametric representations

$$(x(s), y(s)) = \left(\frac{1}{2}(1 + 2 \cos(s) + \cos(2s)), \frac{1}{2}(2 \sin(s) + \sin(2s)) \right)$$

and

$$(x(s), y(s)) = (3 \cos(s) + \cos(3s), 3 \sin(s) - \sin(3s)),$$

which involve trigonometric functions with different arguments, cannot be exactly represented by such a scheme. This explanation should clarify that the exact representation of trigonometric curves of this kind needs the definition of schemes able to reproduce functions from the spaces

$$\{1, x, \cos(sx), \sin(sx), \cos(2sx), \sin(2sx)\} \quad (24)$$

and

$$\{1, x, \cos(sx), \sin(sx), \cos(2sx), \sin(2sx), \cos(3sx), \sin(3sx)\} \quad (25)$$

respectively.

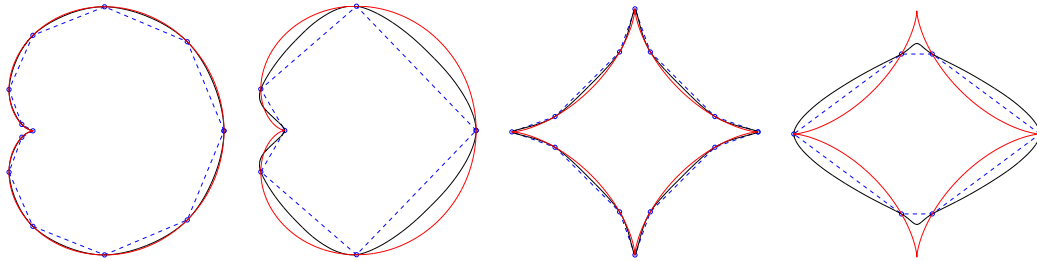


Fig. 1. Comparisons between the cardioid and astroid reconstructions obtained by the scheme in [4] (black lines) and the real plot of these trigonometric curves (red lines). Dashed blue lines denote the chosen starting polygons made respectively of 12 and 6 points sampled at uniform parameter spacings equal to $\frac{\pi}{6}$ and $\frac{\pi}{3}$. As it appears, starting from coarser polylines the difference between the two curves is still more evident.

The following subsections will be devoted to the construction of three novel interpolating 6-point schemes, the second of which turns out to be able to reproduce functions from the space in (24). The explored schemes are all defined over spaces combining algebraic and exponential polynomials, and give rise to different extensions of the space $V_{4,t} = \{1, x, e^{tx}, e^{-tx}\}$ with $t = 0$, $t = s$, or $t = is$, $s > 0$. The first considered superset is the mixed space $V_{6,t} \equiv \{1, x, x^2, x^3, e^{tx}, e^{-tx}\}$, generated by expanding the polynomial part of $V_{4,t}$; the second one is $V_{6,t} \equiv \{1, x, e^{tx}, e^{-tx}, e^{2tx}, e^{-2tx}\}$, obtained by $V_{4,t}$ by adding higher-order exponential functions; the last extension is $V_{6,t} \equiv \{1, x, e^{tx}, e^{-tx}, xe^{tx}, xe^{-tx}\}$, which turns out to be spanned by products of degree-1 algebraic polynomials $1, x$ and order-1 exponential polynomials $1, e^{tx}, e^{-tx}$. As will be shown in Section 5, the three schemes can deal with both C^2 free-form curves and traditional analytical shapes, including conic sections, second-order trigonometric curves, the catenary, the helix and some important spirals. In comparison with the space $V_{4,t}$, which allows an exact representation of standard quadratic and cubic curves only in a limiting case [1],

the first mentioned supraset $V_{6,t}$ can represent parabolas and cubics without resorting to the limit. This property also holds for the second mentioned supraset $V_{6,t}$, because, given an order-1 trigonometric (hyperbolic) function $u(s)$, then $u^2(s)$ is an order-2 trigonometric (hyperbolic). Therefore, the order-2 trigonometric (hyperbolic) curve $(x(s), y(s)) = (u, u^2)$ is a parabola. Anyway, the main advantage of the second space $V_{6,t}$ over $V_{4,t}$, is that it encompasses order-2 trigonometric curves which include several important shapes [9]. Finally, the third mentioned space $V_{6,t}$ deserves our attention since it contains spirals of interest in engineering, such as the circle involute, which represents the curve employed in most gear-tooth profiles.

4.1 An interpolating 6-point C^2 subdivision scheme for conics reproduction

Taking the member of the family $\sigma^k(z)$ in (3) which corresponds to $\ell = 3$ (i.e. $n = 3$), we get the approximating scheme for C^4 exponential B-splines. It is described by the refinement rules

$$\begin{aligned} p_{2j}^{k+1} &= \sigma_1^k p_{j-1}^k + \sigma_3^k p_j^k + \sigma_1^k p_{j+1}^k, \\ p_{2j+1}^{k+1} &= \sigma_0^k (p_{j-1}^k + p_{j+2}^k) + \sigma_2^k (p_j^k + p_{j+1}^k) \end{aligned} \quad (26)$$

with

$$\begin{aligned} \sigma_0^k &= \frac{1}{16(v^{k+1} + 1)}, & \sigma_1^k &= \frac{v^{k+1} + 2}{8(v^{k+1} + 1)}, \\ \sigma_2^k &= \frac{8v^{k+1} + 7}{16(v^{k+1} + 1)}, & \sigma_3^k &= \frac{3v^{k+1} + 2}{4(v^{k+1} + 1)} \end{aligned} \quad (27)$$

where v^{k+1} is updated through (4) for any $k \geq 0$.

We now derive from (26) the corresponding 6-point interpolating scheme following the results presented in Section 3.

Let $\omega^k(z)$ be the degree-4 Laurent polynomial in (16) with coefficients

$$\begin{aligned} \omega_0^k &= \frac{v^{k+1} + 2}{4v^{k+1}(v^{k+1} + 1)}, \\ \omega_1^k &= -\frac{(v^{k+1} + 2)^2}{2v^{k+1}(v^{k+1} + 1)}, \\ \omega_2^k &= \frac{4(v^{k+1})^2 + 9v^{k+1} + 6}{2v^{k+1}(v^{k+1} + 1)} \end{aligned} \quad (28)$$

computed through (19). Hence the associated 6-point interpolating scheme is described by the refinement rules

$$\begin{aligned} p_{2j}^{k+1} &= p_j^k, \\ p_{2j+1}^{k+1} &= \zeta_0^k (p_{j-2}^k + p_{j+3}^k) + \zeta_2^k (p_{j-1}^k + p_{j+2}^k) + \zeta_4^k (p_j^k + p_{j+1}^k) \end{aligned} \quad (29)$$

with

$$\begin{aligned} \zeta_0^k &= \frac{v^{k+1} + 2}{64v^{k+1}(v^{k+1} + 1)^2}, \\ \zeta_2^k &= -\frac{4(v^{k+1})^3 + 8(v^{k+1})^2 + 7v^{k+1} + 6}{64v^{k+1}(v^{k+1} + 1)^2}, \\ \zeta_4^k &= \frac{36(v^{k+1})^3 + 72(v^{k+1})^2 + 38v^{k+1} + 4}{64v^{k+1}(v^{k+1} + 1)^2}. \end{aligned} \quad (30)$$

Due to Corollary 11, it turns out that this scheme can reproduce functions in the space $V_{6,t} \equiv \{1, x, x^2, x^3, e^{tx}, e^{-tx}\}$ for any non-negative real or imaginary constant t . As a consequence, it allows an exact representation of cubics, circles and conic sections, namely of the most important shapes in engineering (see Figures 2 and 3). Note that the coefficients $\{\zeta_{2j}^k\}_{j=0,1,2}$ in (30) are well-defined for any $v^0 \in (-1, +\infty)$. In addition, since when k tends to infinity, v^{k+1} approaches to 1 [1], it follows that

$$\lim_{k \rightarrow +\infty} \zeta_0^k = \frac{3}{256}, \quad \lim_{k \rightarrow +\infty} \zeta_2^k = -\frac{25}{256}, \quad \lim_{k \rightarrow +\infty} \zeta_4^k = \frac{75}{128}, \quad (31)$$

and hence the scheme (29)-(30)-(4) brings back to the stationary 6-point scheme in [19]. By Theorem 2.5 in [7] the 6-point interpolating scheme with coefficients in (30) is the only 6-point reproducing the space $V_{6,t}$. Thus, Theorems 2.7 and 2.10 in [7] allow us to claim C^2 smoothness of the proposed 6-point scheme for any choice of the starting parameter v^0 in the range $(-1, +\infty)$. Because such a scheme encompasses under unified rules both C^2 free-form and traditional analytical shapes, it provides an important improvement of the existing interpolating subdivision schemes, which are either C^1 and able to reproduce such a family of curves ([1], [4], [8], [20] and [21]), or C^2 but not able to reproduce any kind of fundamental shapes except cubic polynomials ([2], [19]).

In the following subsection we will show how to generate exactly trigonometric curves of the second-order (i.e. described by means of parametric equations involving order-2 trigonometric functions) by an interpolating 6-point scheme derived straightforwardly from the $\ell = 3$ (i.e. $n = 2$) member of the approximating family in (9).

4.2 *An interpolating 6-point C^2 subdivision scheme for second-order curves reproduction*

Let us consider the approximating scheme described by the Laurent polynomial $\sigma^k(z)$ in (9) when setting $\ell = 3$ (i.e. $n = 2$). The associated refinement rules are given by equations (26) with

$$\begin{aligned}\sigma_0^k &= \frac{1}{16(v^{k+1})^2(v^{k+1} + 1)}, & \sigma_1^k &= \frac{2v^{k+1} + 1}{8v^{k+1}(v^{k+1} + 1)}, \\ \sigma_2^k &= \frac{8(v^{k+1})^3 + 8(v^{k+1})^2 - 1}{16(v^{k+1})^2(v^{k+1} + 1)}, & \sigma_3^k &= \frac{4(v^{k+1})^2 + 2v^{k+1} - 1}{4v^{k+1}(v^{k+1} + 1)}\end{aligned}\tag{32}$$

where v^{k+1} is updated through (4) for all $k \geq 0$.

Like before, we construct the degree-4 Laurent polynomial $\omega^k(z)$ by computing its coefficients

$$\begin{aligned}\omega_0^k &= \frac{2v^{k+1} + 1}{4(v^{k+1} + 1)(2v^{k+1} - 1)[2(v^{k+1})^2 - 1]}, \\ \omega_1^k &= -\frac{v^{k+1}(2v^{k+1} + 1)^2}{2(v^{k+1} + 1)(2v^{k+1} - 1)[2(v^{k+1})^2 - 1]}, \\ \omega_2^k &= \frac{8(v^{k+1})^4 + 12(v^{k+1})^3 - 2v^{k+1} + 1}{2(v^{k+1} + 1)(2v^{k+1} - 1)[2(v^{k+1})^2 - 1]}\end{aligned}\tag{33}$$

through formula (19). Hence the associated 6-point interpolating scheme is described by the refinement rules in (29) with

$$\begin{aligned}\zeta_0^k &= \frac{2v^{k+1} + 1}{64(v^{k+1})^2(v^{k+1} + 1)^2(2v^{k+1} - 1)[2(v^{k+1})^2 - 1]}, \\ \zeta_2^k &= -\frac{[4(v^{k+1})^2 + 2v^{k+1} - 1]^2}{64(v^{k+1})^2(v^{k+1} + 1)^2[2(v^{k+1})^2 - 1]}, \\ \zeta_4^k &= \frac{(2v^{k+1} + 1)[4(v^{k+1})^2 + 2v^{k+1} - 1]^2}{32(v^{k+1})^2(v^{k+1} + 1)^2(2v^{k+1} - 1)}.\end{aligned}\tag{34}$$

Due to Corollary 11, it turns out that this scheme can reproduce functions from the space $V_{6,t} \equiv \{1, x, e^{tx}, e^{-tx}, e^{2tx}, e^{-2tx}\}$ for any non-negative real or imaginary constant t . As a consequence, algebraic curves of the second-order, such as the cardioid, Pascal's limaçon, the deltoid, the piriform, Geronon's lemniscate, the eight

curve, and the 3-dimensional Viviani's curve (see Figures 5 and 7-(b)) can be exactly generated. Note that the coefficients $\{\zeta_{2j}^k\}_{j=0,1,2}$ in (34) are well-defined for any $v^0 \in (-1, +\infty) \setminus \{-\frac{1}{2}, 0\}$. In addition, since (31) still holds and by Theorem 2.5 in [7] the 6-point interpolating scheme with the so computed coefficients turns out to be the only one reproducing the above space $V_{6,t}$, C^2 smoothness of the scheme (29)-(34)-(4) for any choice of the starting parameter v^0 in the range $(-1, +\infty) \setminus \{-\frac{1}{2}, 0\}$, follows from Theorems 2.7 and 2.10 in [7]. Thus the refinement rules (29)-(34)-(4) turn out to be unique in combining the fundamental property of C^2 smoothness with the ability to reproduce such a kind of second-order algebraic curves considered of great interest in applications.

In the following subsection we will show how to exactly generate plane and space spirals playing a relevant role in engineering, by means of an interpolating 6-point scheme derived straightforwardly from the $\ell = 3$ (i.e. $n = 2$) member of the approximating family in (13).

4.3 An interpolating 6-point C^2 subdivision scheme for spirals reproduction

Let us consider the approximating scheme described by the Laurent polynomial $\sigma^k(z)$ in (13) when setting $\ell = 3$ (i.e. $n = 2$). The associated refinement rules are given by equations (26) with

$$\begin{aligned} \sigma_0^k &= \frac{1}{8(v^{k+1} + 1)^2}, & \sigma_1^k &= \frac{2v^{k+1} + 1}{4(v^{k+1} + 1)^2}, \\ \sigma_2^k &= \frac{4(v^{k+1})^2 + 8v^{k+1} + 3}{8(v^{k+1} + 1)^2}, & \sigma_3^k &= \frac{2(v^{k+1})^2 + 2v^{k+1} + 1}{2(v^{k+1} + 1)^2} \end{aligned} \quad (35)$$

where v^{k+1} is updated through (4) for all $k \geq 0$.

Like before, we construct the degree-4 Laurent polynomial $\omega^k(z)$ by computing its coefficients

$$\begin{aligned} \omega_0^k &= \frac{2v^{k+1} + 1}{8(v^{k+1})^3}, \\ \omega_1^k &= -\frac{(2v^{k+1} + 1)^2}{4(v^{k+1})^3}, \\ \omega_2^k &= \frac{4(v^{k+1})^3 + 8(v^{k+1})^2 + 6v^{k+1} + 1}{4(v^{k+1})^3} \end{aligned} \quad (36)$$

through formula (19). Hence the associated 6-point interpolating scheme is described by the refinement rules in (29) with

$$\begin{aligned}
\zeta_0^k &= \frac{2v^{k+1} + 1}{64(v^{k+1})^3(v^{k+1} + 1)^2}, \\
\zeta_2^k &= -\frac{(4v^{k+1} + 1)[4(v^{k+1})^2 + 2v^{k+1} - 1]}{64(v^{k+1})^3(v^{k+1} + 1)^2}, \\
\zeta_4^k &= \frac{(2v^{k+1} + 1)[2(v^{k+1})^2 + 2v^{k+1} + 1][4(v^{k+1})^2 + 2v^{k+1} - 1]}{32(v^{k+1})^3(v^{k+1} + 1)^2}.
\end{aligned} \tag{37}$$

Due to Corollary 11, it turns out that this scheme can reproduce functions from the space $V_{6,t} \equiv \{1, x, e^{tx}, e^{-tx}, xe^{tx}, xe^{-tx}\}$ for any non-negative real or imaginary constant t . As a consequence, spirals like the circle involute, the Archimedean spiral and the 3-dimensional conical spiral (see Figures 6 and 7-(c)) can be exactly generated. Note that the coefficients $\{\zeta_{2j}^k\}_{j=0,1,2}$ in (37) are well-defined for any $v^0 \in (-1, +\infty)$. In addition, since (31) still holds and by Theorem 2.5 in [7] the 6-point interpolating scheme with the so computed coefficients turns out to be the only one reproducing the above space $V_{6,t}$, C^2 smoothness of the scheme (29)-(37)-(4) for any choice of the starting parameter v^0 in the range $(-1, +\infty)$, follows from Theorems 2.7 and 2.10 in [7]. Thus, the refinement rules in (29)-(37)-(4) turn out to be unique in combining the fundamental property of C^2 smoothness with the ability to generate spirals deserving a special attention in applications as employed in most gear-tooth profiles.

5 Numerical examples

In this section we illustrate the most important trigonometric and transcendental curves that can be reproduced by the interpolatory 6-point schemes introduced before.

Figures 2, 3 and 4 depict the plane curves that can be encompassed by all the three schemes in Section 4.

Figure 5 depicts some classical second-order plane curves (such as the cardioid, Pascal's limaçon, the deltoid, the piriform, Geronon's lemniscate and the eight curve) that admit an exact representation by means of the interpolating 6-point scheme in Subsection 4.2.

Figure 6 depicts the reproduction of the circle involute and the Archimedean spiral via the interpolating 6-point scheme in Subsection 4.3.

Figure 7 shows the exact reconstruction of trigonometric space curves through the interpolating 6-point schemes presented in Subsections 4.1, 4.2 and 4.3. While the helix (Figure 7-(a)) can be reproduced by all the three schemes, the Viviani's curve

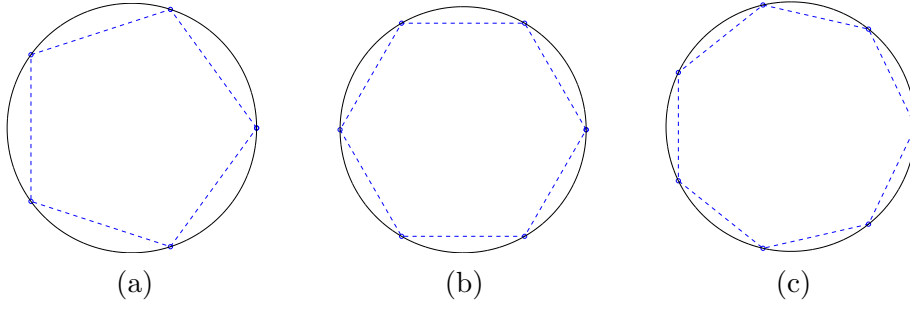


Fig. 2. Reconstruction of exact circles through the interpolating 6-point schemes presented in Subsections 4.1, 4.2 and 4.3. Dashed lines depict the regular κ -gons (with $\kappa = 5, 6, 7$) assumed as starting polygons. The corresponding initial parameter is respectively chosen as (a) $v^0 = \cos\left(\frac{2\pi}{5}\right)$, (b) $v^0 = \frac{1}{2}$, (c) $v^0 = \cos\left(\frac{2\pi}{7}\right)$.

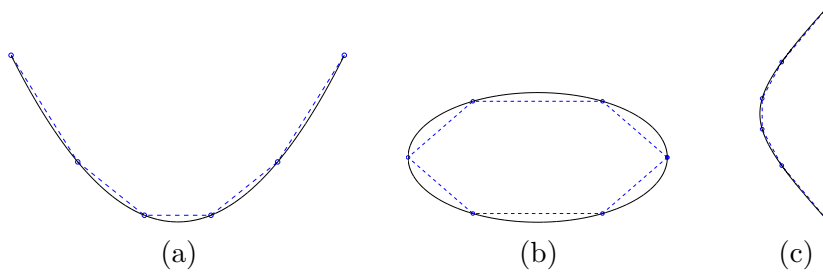


Fig. 3. Exact reconstruction of conic sections through the interpolating 6-point schemes presented in Subsections 4.1, 4.2 and 4.3. Dashed lines depict the assumed starting polygons. The corresponding initial parameter is respectively chosen as (a) $v^0 = 1$, (b) $v^0 = \frac{1}{2}$, (c) $v^0 = \cosh\left(\frac{3}{5}\right)$.

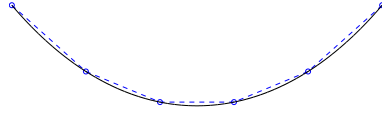


Fig. 4. Exact reconstruction of the catenary through the interpolating 6-point schemes presented in Subsections 4.1, 4.2 and 4.3. The dashed line depicts the assumed starting polygon. The corresponding initial parameter is chosen as $v^0 = \cosh\left(\frac{2}{5}\right)$.

(Figure 7-(b)) and the conical spiral (Figure 7-(c)) have been generated through the refinement rules in Subsections 4.2 and 4.3 respectively.

Finally, in Figures 8, 9, 10 we give examples of interpolatory C^2 free-form curves exhibiting increasing tensions in correspondence of progressively increasing values of v^0 in $(-1, +\infty)$. Note how, depending on the scheme, the limit curve differently shrinks to the starting polyline.

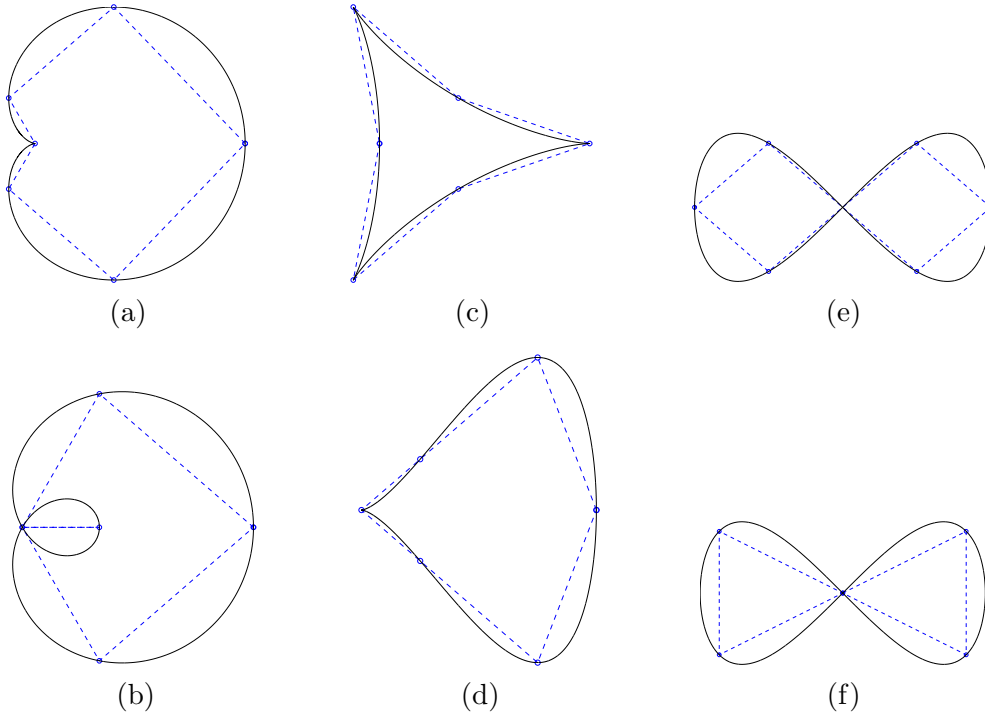


Fig. 5. Exact reconstruction of the cardioid (a), Pascal's limaçon (b), the deltoid (c), the piriform (d), the lemniscate of Geronno (e) and the eight curve (f) through the interpolating 6-point scheme in Subsection 4.2 with starting parameter $v^0 = \frac{1}{2}$. Dashed lines denote the chosen starting polygons made of 6 points sampled at a uniform parameter spacing of $\frac{\pi}{3}$.

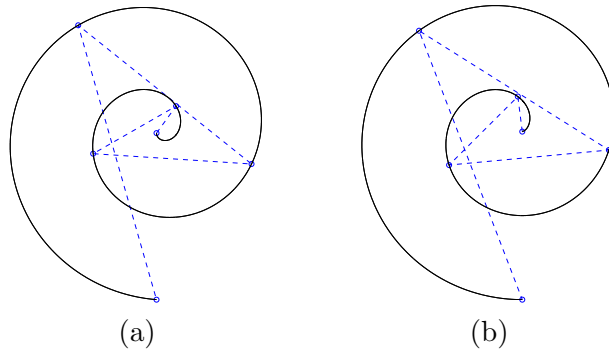


Fig. 6. Exact reconstruction of the Archimedean spiral (a) and of the circle involute (b) through the interpolating 6-point scheme in Subsection 4.3 with starting parameter $v^0 = \cos\left(\frac{4\pi}{5}\right)$. Dashed lines denote the chosen starting polygons made of 6 points sampled at a uniform parameter spacing of $\frac{4\pi}{5}$.

As a closing remark, we let the reader observe that, when the starting sequence of control points is non-uniformly spaced, the non-stationary interpolatory 4-point and 6-point schemes generate limit curves of a better quality than the ones obtained by the Dubuc-Deslauriers 4-point and by the Weissmann 6-point schemes (Figure 11). However, they are not artifact free. In fact, when the initial control polygon

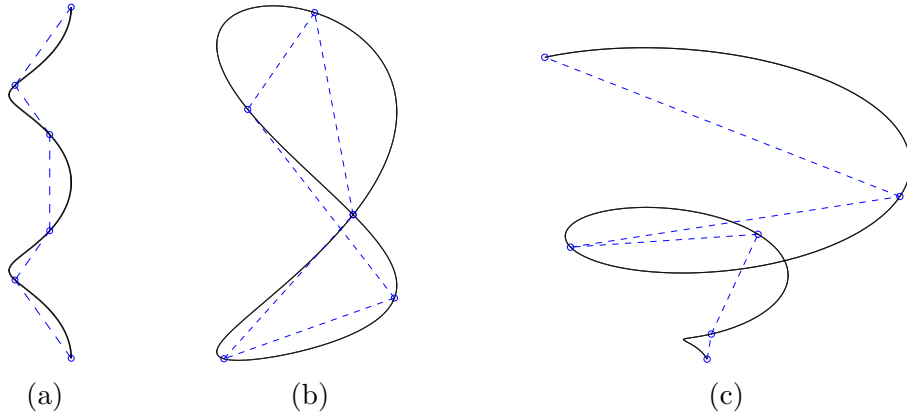


Fig. 7. Exact reconstruction of trigonometric space curves through the interpolating 6-point schemes presented in Subsections 4.1, 4.2 and 4.3. Dashed lines depict the assumed starting polygons. The corresponding initial parameter is chosen respectively as: (a) $v^0 = \cos\left(\frac{4\pi}{5}\right)$, (b) $v^0 = \cos\left(\frac{2\pi}{5}\right)$, (c) $v^0 = \cos\left(\frac{4\pi}{5}\right)$.

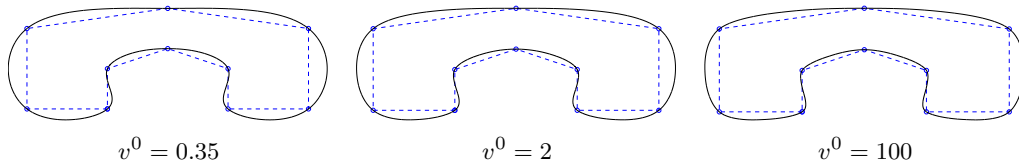


Fig. 8. The effect of subdividing the same starting polygon with the interpolating 6-point scheme in Subsection 4.1 starting from different initial tension values.

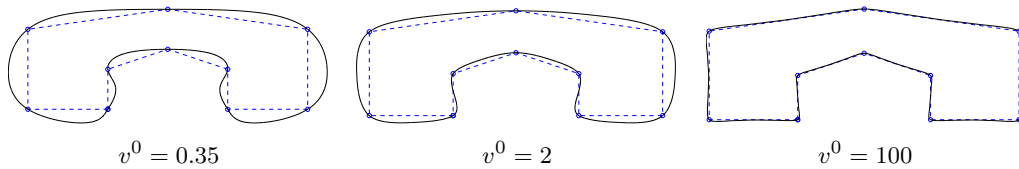


Fig. 9. The effect of subdividing the same starting polygon with the interpolating 6-point scheme in Subsection 4.2 starting from different initial tension values.

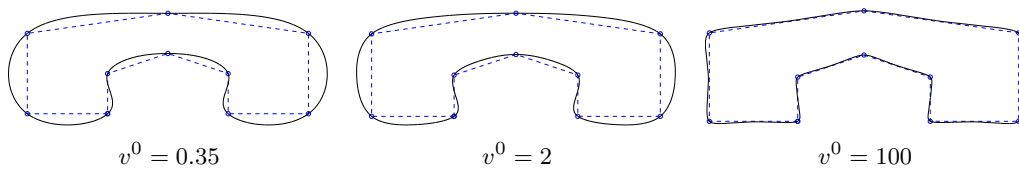


Fig. 10. The effect of subdividing the same starting polygon with the interpolating 6-point scheme in Subsection 4.3 starting from different initial tension values.

has edges of highly non-uniform length, undesired oscillations usually occur in the limit curve (Figure 12).

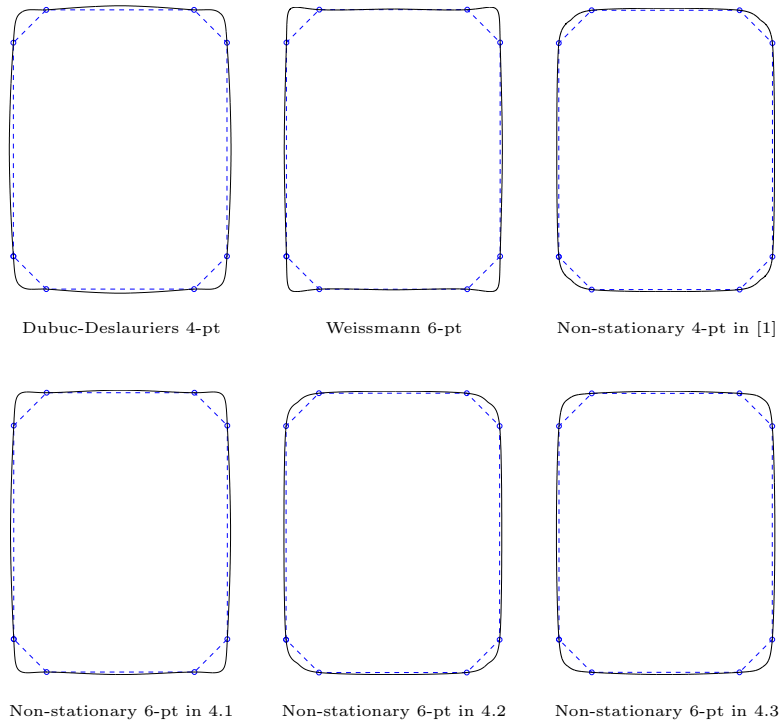


Fig. 11. Comparison between limit curves obtained by subdividing the same sequence of non-uniformly spaced control points through the stationary interpolating 4-point and 6-point schemes and through the non-stationary interpolating 4-point and 6-point schemes with parameter $v^0 = 4$.

6 Conclusions

At present, the algorithms for producing curves which appear to be the most efficient, flexible, and easy to implement, are given by subdivision schemes.

However, in spite of the numerous proposals that are continuously appearing in the literature, none is still able to combine simplicity of definition and implementation, with the generation of C^2 limit curves featured by a user-controllable distance from the starting polyline as well as by the potentiality of representing exactly a wide variety of fundamental shapes of great interest in engineering and CAGD applications.

To this purpose, in this paper we have presented three different families of approximating subdivision schemes generating piecewise exponential polynomials and we have proposed a general strategy for turning them into 2ℓ -point interpolating schemes able to reproduce functions in the same spaces.

The interpolating 6-point schemes derived in Section 4 offer examples of how this can be done and show how the proposed approach can generate curve subdivision algorithms that compare favorably with all the interpolating schemes appeared in the literature up to now. In fact, they all allow defining fully automatic interpolatory schemes with C^2 smoothness, that turn out to be both tension-controlled and

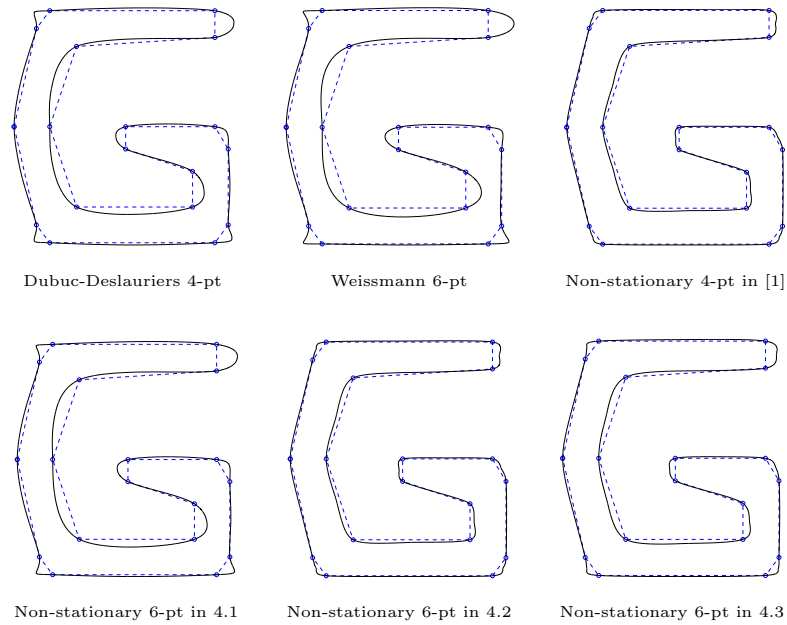


Fig. 12. Limit curves obtained by subdividing an initial control polygon with edges of highly non-uniform length through the stationary interpolating 4-point and 6-point schemes and through the non-stationary interpolating 4-point and 6-point schemes with parameter $v^0 = 7$.

able to reproduce salient trigonometric and transcendental curves often needed in CAGD and its applications.

7 Acknowledgements

This research was supported by University of Milano-Bicocca, Italy. The author thanks the anonymous referees for their careful reading of the manuscript and for their valuable comments.

References

- [1] C. Beccari, G. Casciola, L. Romani, A non-stationary uniform tension controlled interpolating 4-point scheme reproducing conics, *Computer Aided Geometric Design* 24(1) (2007) 1-9.
- [2] C. Beccari, G. Casciola, L. Romani, An interpolating 4-point C^2 ternary non-stationary subdivision scheme with tension control, *Computer Aided Geometric Design* 24(4) (2007) 210-219.

- [3] Q.Y. Chen, G.Z. Wang, A class of Bézier-like curves, *Computer Aided Geometric Design* 20 (2003) 29-39.
- [4] S. Daniel, P. Shunmugaraj, Some non-stationary subdivision schemes, *Geometric Modelling and Imaging (GMAI'07)*, 2007, pp. 33-38.
- [5] G. Deslauriers, S. Dubuc, Symmetric iterative interpolation processes, *Constr. Approx.* 5 (1989) 49-68.
- [6] S. Dubuc, Interpolation through an iterative scheme, *J. Math. Anal. Appl.* 114 (1986) 185-204.
- [7] N. Dyn, D. Levin, A. Luzzatto, Exponentials reproducing subdivision schemes, *Found. Comput. Math.* 3 (2003) 187-206.
- [8] M.K. Jena, P. Shunmugaraj, P.C. Das, A non-stationary subdivision scheme for curve interpolation, *Anziam J.* 44(E) (2003) 216-235.
- [9] J.D. Lawrence, *A catalog of special plane curves*, Dover, New York, 1972.
- [10] G. Li, W. Ma, A method for constructing interpolatory subdivision schemes and blending subdivisions, *Computer Graphics Forum* 26(2) (2007) 185-201.
- [11] Y.-J. Li, G.-Z. Wang, Two kinds of B-basis of the algebraic hyperbolic space, *J. of Zhejiang University Science* 6A(7) (2005) 750-759.
- [12] Y. Lü, G. Wang, X. Yang, Uniform hyperbolic polynomial B-spline curves, *Computer Aided Geometric Design* 19 (2002) 379-393.
- [13] E. Mainar, J.M. Peña, J. Sanchez-Reyes, Shape preserving alternatives to the rational Bézier model, *Computer Aided Geometric Design* 18 (2001) 37-60.
- [14] E. Mainar, J.M. Peña, A basis of C-Bézier splines with optimal properties, *Computer Aided Geometric Design* 19 (2002) 161-175.
- [15] G. Morin, J. Warren, H. Weimer, A subdivision scheme for surfaces of revolution, *Computer Aided Geometric Design* 18 (2001) 483-502.
- [16] L.L. Schumaker, *Spline functions: basic theory*, Wiley, New York, 1981.
- [17] G. Wang, M. Fang, Unified and extended form of three types of splines, to appear in *Journal of Computational and Applied Mathematics* (2007).
- [18] J. Warren, H. Weimer, *Subdivision methods for geometric design*, Morgan Kaufmann (2002).
- [19] A. Weissmann, A 6-point interpolating subdivision scheme for curve design, M. Sc. Thesis, Tel-Aviv University, 1990.
- [20] J. Zhang, F.-L. Krause, Extending cubic uniform B-splines by unified trigonometric and hyperbolic basis, *Graphical Models* 67 (2005) 100-119.
- [21] J. Zhang, F.-L. Krause, H. Zhang, Unifying C-curves and H-curves by extending the calculation to complex numbers, *Computer Aided Geometric Design* 22(9) (2005) 865-883.